

Application of radial basis functions to shape description in a dual-element off-axis magnifier

Ozan Cakmakci,^{1,*} Sophie Vo,¹ Hassan Foroosh,² and Jannick Rolland^{1,2}

¹CREOL, The College of Optics and Photonics, University of Central Florida, Orlando, Florida 32816, USA

²School of Electrical Engineering and Computer Science, University of Central Florida, Orlando, Florida 32816, USA

*Corresponding author: ozan.cakmakci@gmail.com

Received December 19, 2007; revised April 4, 2008; accepted April 6, 2008;
posted April 25, 2008 (Doc. ID 90975); published May 29, 2008

We previously demonstrated that radial basis functions may be preferred as a descriptor of free-form shape for a single mirror magnifier when compared to other conventional descriptions such as polynomials [Opt. Express **16**, 1583 (2008)]. A key contribution is the application of radial basis functions to describe and optimize the shape of a free-form mirror in a dual-element magnifier with the specific goal of optimizing the pupil size given a 20° field of view. We demonstrate a 12 mm exit pupil, 20° diagonal full field of view, 15.5 mm eye clearance, 1.5 arc min resolution catadioptric dual-element magnifier design operating across the photopic visual regime. A second contribution is the explanation of why it is possible to approximate any optical mirror shape using radial basis functions. © 2008 Optical Society of America

OCIS codes: 220.2740, 220.4830, 050.1970.

The design of compact magnifiers is important in applications such as mobile information displays. Applications of the design presented in this Letter are personal information management, reading or writing notes and e-mails, watching multimedia content, and visual overlays assisting the task at hand. The optical magnifier presented in this Letter is intended to be coupled monocularly or binocularly with the human visual system under photopic conditions.

Our approach is to consider a catadioptric dual-element magnifier design and explore its performance and pupil size limits for a fixed field of view. The catadioptric design comprises a free-form mirror and an aspheric mirror with a diffractive surface. We are using the term free-form in reference to surfaces that are rotationally nonsymmetric. Examples of free-form surface descriptions include x - y polynomials and Zernike polynomials. In terms of fabrication feasibility, we have successfully fabricated magnifiers based on an x - y polynomial surface description using diamond-turning technology [1]. Furthermore, the design is an off-axis magnifier, which folds the optical axis around the human head while providing the necessary clearances. The symmetry around the ray connecting the centers of the image, object, pupils, and vertices of the elements is broken because of the asymmetries in the free-form mirror classifying this system as off-axis. In this off-axis design, it is necessary to minimize the fold angle to keep the incidence angles of the rays on the mirror as small as possible. Achieving a minimum element count magnifier is a highly constrained problem, making the shape of the free-form surface a key variable to optimize.

We demonstrated in our previous work (a) an 8 mm exit pupil, 20° diagonal full field of view, 15 mm eye clearance, 1.5 arc min resolution catadioptric dual-element magnifier design operating across the photopic visual regime [1]; and (b) that radial basis functions may be preferred as a description of free-form shape when compared to other conventional descriptions such as polynomials [2].

The two new contributions in this Letter are (a) the application of a sum of local basis functions for the description of the free-form mirror in the dual-element design, with a primary goal being to expand the pupil size from 8 [1] to 12 mm, while keeping the same level of modulation transfer function (MTF) performance; and (b) the explanation of why it is possible to approximate any optical mirror shape using radial basis functions.

To date, the majority of aspherical shape descriptions have relied on global polynomials, for example, Zernike polynomials. The related work, which is directly connected to the work presented in this Letter, comes in part from the antenna design community where Chan *et al.* [3] analyzed the fit errors of a known function represented by radial basis functions, and in part from wave propagation theory where Reynolds decomposed wavefronts into a linear combination of 1D Gaussians [4]. Some of the theoretical foundations of radial basis functions reside within the literature of neural networks and mathematics [5,6]. In summarizing the framework below we are interested in two related questions in the context of this Letter. First, whether it is possible to approximate any surface shape using this framework (i.e., universal approximation property). Second, what is the criteria that the basis functions need to satisfy so that the span of linear combinations of translated basis functions will contain any optical surface shape?

An optical surface can be represented by a linear combination of basis functions added to a base conic as

$$z(x,y) = \frac{c(x^2 + y^2)}{1 + \sqrt{1 - (1+k)c^2(x^2 + y^2)}} + \sum_n \phi_n w_n. \quad (1)$$

The only advantage to representing the departure from a base conic is in the use of current software, in that the computation of paraxial quantities is based on the base conic. The base conic is dropped there-

after. The Wiener approximation theorem [7] states that the translates, $\phi(x+x_0)$, of a function $\phi(x)$ are dense in L^2 (i.e., the set of all measurable functions that are square-integrable forms—the so-called L^2 space) given that $\hat{\phi}(w) \neq 0$, where

$$\hat{\phi} = \frac{1}{\sqrt{2\pi}} \int_{-\infty}^{\infty} \phi(x) e^{-iwx} dx, \quad (2)$$

is the Fourier transform of $\phi(x)$. Dense in L^2 means that linear combinations of translated functions will span L^2 . A surface of finite extent can be described as a finite vector and thus resides in L^2 . The significance of the Wiener approximation theorem is to ensure that we can approximate any shape using a linear combination of basis functions that have nonvanishing Fourier transforms. In the case where the function $\phi(x)$ belongs to the set of radial basis functions, the surface Z can be written as

$$z(\mathbf{x}) = \sum_n \phi_n(\|\mathbf{x} - \mathbf{c}_n\|) \mathbf{w}_n, \quad (3)$$

where \mathbf{x} is a vector of x - y locations on the aperture, \mathbf{c} is a vector containing the centers of the radial basis functions, \mathbf{w} is a vector of weights, and $\|\cdot\|$ denotes the Euclidean norm. Examples of radial basis functions with nonvanishing Fourier transforms include a Gaussian, a thin-plate spline, and a multiquadric [8].

In this Letter, we report on our choice of two-dimensional (2D) Gaussians as the basis functions denoted as $\phi(\mathbf{x})$, where \mathbf{x} is a vector. Gaussians possess several desirable properties from the point of view of optical design. First, Gaussians are smooth functions (C^∞) having derivatives of all orders providing a desirable property given that optical surfaces are smooth. In addition, smoothness is desirable from a fabrication point of view. Second, theoretically, Gaussians are not local functions; however, practically, they can be considered local since the value of a Gaussian outside of 3σ is small (<0.011 , for a unit amplitude Gaussian). Third, the Fourier transform of a Gaussian is a Gaussian that provides an analytical description for the power spectral density (PSD) of the surface. Hartman *et al.* provided a proof of the universal approximation property of radial basis function networks with Gaussian basis functions [5]. The proof of Hartman *et al.* [5] guarantees that there will be a Gaussian radial basis function network, for any ε , where the difference between the original function and its approximation is such that $|f(x) - \hat{f}(x)| < \varepsilon$ (i.e., arbitrarily well approximation). This proof answers the question of why it is possible to describe any mirror shape using Gaussian radial basis functions.

Figure 1 shows a three-layer radial basis function network (RBFN) that is used in this Letter to represent a rotationally nonsymmetric free-form optical mirror. The first layer consists of the inputs, which are the x and y locations along the aperture. The inputs are connected to the second layer comprising nonlinear basis functions, each with a unique center. The linear combinations of these basis functions

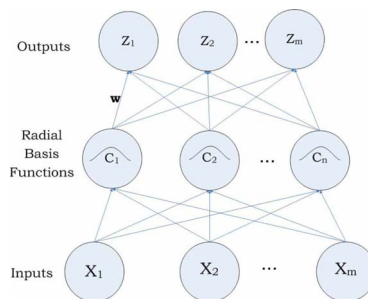


Fig. 1. (Color online) Three-layer radial basis function network.

evaluated at the distance between the input and the basis center form the third layer consisting of the outputs. The vector \mathbf{w} contains the weights of the linear combinations. We can observe, for example, in a network representation that there is no interdependence between the basis functions shown in layer 2. The number of basis functions does not have to equal the number of inputs and it is preferable to have fewer basis functions compared to the inputs. The centers of the radial basis functions need not be coincident with the inputs. Each basis can have its own width σ . A bias parameter can be incorporated into the second layer. The network in Fig. 1 can be represented in matrix form as

$$\Phi \mathbf{w} = Z, \quad (4)$$

where Φ is an $m \times n$ matrix, \mathbf{w} is a vector of weights, and Z is the resulting surface. Each column in the Φ matrix contains a nonlinear basis function.

We apply the Gaussian radial basis functions to a dual-element magnifier comprising a free-form mirror and a lens with a diffractive optical element. The starting point for the design was the dual-element magnifier previously reported [1]. We implemented the radial basis functions as a user-defined type 1 surface in the optical design software Code V as a dynamically linked library. Code V interacts with a surface one ray at a time, which reduces the Φ matrix to a row; therefore, the sag of each point on the surface becomes a dot product. We used Code V to optimize the mirror shape while increasing the pupil from 8 mm in the starting point design to the maximum achievable pupil as determined by an MTF value of 20% at the Nyquist frequency. The optimizer attempts to minimize a merit function, which in our case is the root mean square of the transverse ray errors measured from their respective reference wavelength chief rays. The results presented in this Letter are for a mirror surface described by a uniformly spaced grid of 16×16 2D unit variance Gaussian functions (i.e., 1 mm variance in the x and y directions over a mirror aperture diameter of ~ 20 mm) shown in Fig. 2(a). A corollary of the Wiener approximation theorem is that it holds regardless of the choice of variances in the case of Gaussian translates. Optimal selection of the variance value and grid size will be addressed in future work. Before optimization, we set the weights in Eq. (1), \mathbf{w}_i , to zero. The optimization constraints included the focal

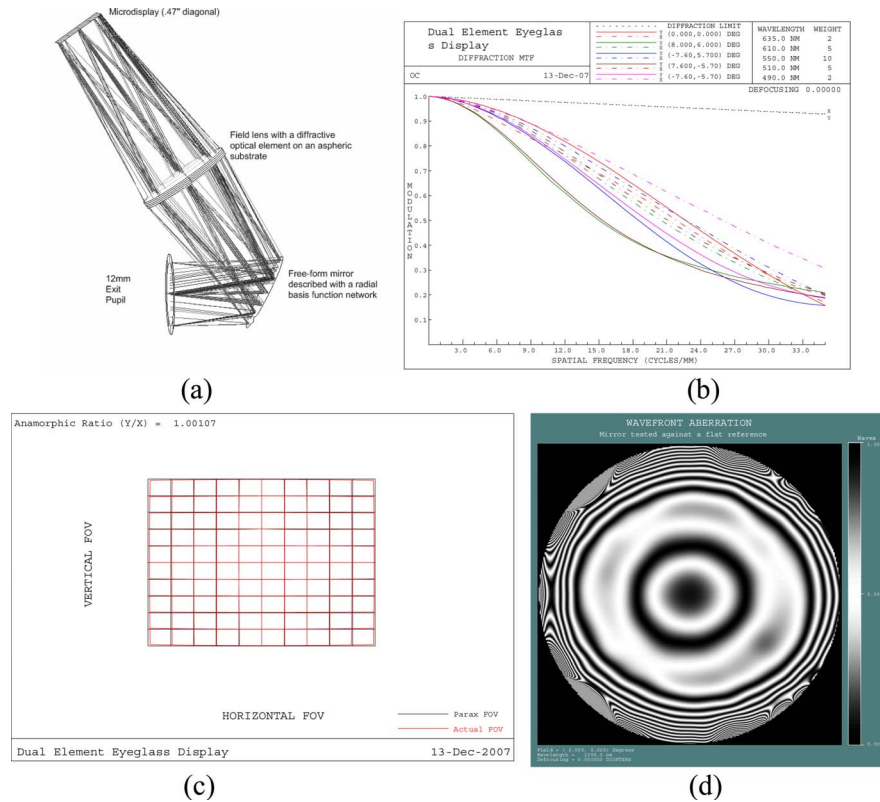


Fig. 2. (Color online) (a) Optical layout of the dual-element magnifier. (b) MTF of the dual-element solution evaluated with a 12 mm pupil. (c) Distortion grid comparing real and paraxial rays ($<2\%$ maximum distortion). (d) Interferogram of the mirror surface represented with radial basis functions.

length, image distortion, and eye clearance. The optimization variables included the two base curvatures of the lens, the aspheric coefficients up to the tenth order on the lens surface facing the mirror, the rotationally symmetric polynomial coefficients up to the eighth order describing the superimposed diffractive optical surface, the image plane defocus, eye clearance, and the 256 weights for the 16×16 2D Gaussian basis functions. The base curvature for the final design was ~ 1 m and was not varied during optimization. We achieved a pupil size of 12 mm.

Figure 2(a) shows the layout of the dual-element off-axis catadioptric magnifier where the mirror is described with Gaussian radial basis functions. A red, blue, and green microdisplay pixel triplet is $15 \mu\text{m}$ in size, which yields a Nyquist frequency of ~ 33 cycles/mm. Thus the polychromatic MTF is plotted up to 35 cycles/mm. Under photopic illumination the pupil of the human eye is ~ 3 mm, and it is customary to conduct the analysis for a 3 mm eye pupil for both centered and decentered pupils. The polychromatic MTF evaluated for a centered 12 mm pupil is plotted in Fig. 2(b) for the performance-limiting fields. In the case of a 3 mm pupil, the lowest MTF value at the Nyquist frequency is $\sim 50\%$. In the current prototype, the microdisplay has a ~ 12 mm diagonal and contains 640×480 pixels. In visual space, the display provides 1.5 arc min resolution as limited by the pixel spacing on the microdisplay, which approaches the human visual acuity of 1 arc min set by a $2.5 \mu\text{m}$ cone spacing. The maximum distortion oc-

currs at $(x=-8^\circ, y=-6^\circ)$ in the field and was measured in simulation to be -1.83% . Figure 2(c) shows the appearance of a rectilinear grid as viewed through the magnifier. Figure 2(d) shows an interferogram of the mirror surface compared to a flat reference wavefront.

We would like to conclude with the practical significance of a 12 mm exit pupil within a distortion-free design, which allows the construction of a stereo display without moving parts for interpupillary distance adjustment, simplifying the optomechanical design of the display assembly and resulting in a robust system.

This work was supported by the Link Foundation, the FPCE, Optical Research Associates, and the National Science Foundation grant IIS/HCI 03-07189.

References

- O. Cakmakci and J. P. Rolland, *Opt. Lett.* **32**, 1363 (2007).
- O. Cakmakci, B. Moore, H. Foroosh, and J. Rolland, *Opt. Express* **16**, 1583 (2008).
- A. K. Chan, C. K. Chui, and L. T. Guan, *Proc. SPIE* **1251**, 62 (1990).
- A. Reynolds, *Proc. SPIE* **560**, 33 (1985).
- E. J. Hartman, J. D. Keeler, and J. M. Kowalski, *Neural Comput.* **2**, 210 (1990).
- S. Bochner, *Math. Ann.* **108**, 378 (1933).
- N. Wiener, *The Fourier Integral and Certain of Its Applications* (Cambridge U. Press, 1933).
- M. D. Buhmann, *Radial Basis Functions: Theory and Implementations* (Cambridge U. Press, 2003).